

Passive seismic imaging with noise sources in complex medium

Deyan Draganov and Kees Wapenaar

Section of Applied Geophysics and Petrophysics, Centre for Technical Geoscience, Delft University of Technology, The Netherlands (Corresponding author d.s.draganov@citg.tudelft.nl)

SUMMARY

Passive seismic imaging is a method to image the subsurface making use of the presence in it of noise sources of seismic waves. The method is based on the relation between the reflection and transmission responses of a medium. This relation states in general that the reflection response of a medium and its time-reversal equal minus the cross-correlation of the measured transmission responses from the subsurface sources plus a delta function. Having in mind that the reflection data is causal a function of time, to obtain the reflection response in practice we just mute the time-reversed part. Having received the simulated reflection response of the subsurface after the cross-correlation process, one can apply on it the standard processing sequence, finishing with migration, for obtaining a final image of the subsurface. Another possibility is to apply a shot-profile migration scheme directly on the recorded transmission data. The result is a migrated image of the subsurface, which is identical to the result of the migration of the simulated reflection responses. The application of one or the other method to obtain the migrated result depends on the set goals.

The quality of both the reconstructed reflection and the reconstructed depth image depend on the characteristics of the recorded transmission signals. Numerical modelling showed that with smaller number of subsurface sources the quality of the reconstructed reflection drops fast, while the reconstruction of the depth image still delivers good results. Another characteristic of the recorded transmission is its duration. In case of white noise sources in the subsurface, when shortening the duration of the recorded transmissions, the quality of the reconstructed reflection drops significantly, while again the reconstructed depth image shows much better results.

KEY WORDS: Passive seismic imaging, daylight imaging, migration, transmission response, reflection response

INTRODUCTION

The method of passive seismic imaging of the subsurface was first proposed by Claerbout (1968), where he showed that by auto-correlating the transmission response of a 1-D acoustic medium measured at the surface, one obtains the reflection response of the same medium. He named this method Acoustic Day-

light Imaging. Later, he stated the conjecture that in the case of a 3-D medium, to simulate the reflection response one needs to cross-correlate the measured transmission responses. In 2002, Wapenaar proved mathematically this conjecture (Wapenaar et al., 2002) for 3-D inhomogeneous acoustic medium.

ACOUSTIC DAYLIGHT IMAGING

Relation between reflection and transmission

In Wapenaar et al. (2004) general relations are given for the reflection and the transmission responses of a 3-D inhomogeneous medium. One of the relations is used in the acoustic daylight imaging:

$$R^+(\mathbf{x}_A, \mathbf{x}_B, \omega) + \{R^+(\mathbf{x}_A, \mathbf{x}_B, \omega)\}^* = \delta(\mathbf{x}_{H,A} - \mathbf{x}_{H,B}) - \int_{\partial\mathcal{D}_m} T^-(\mathbf{x}_A, \mathbf{x}, \omega) \{T^-(\mathbf{x}_B, \mathbf{x}, \omega)\}^* d^2\mathbf{x} . \quad (1)$$

In the above equation $R^+(\mathbf{x}_A, \mathbf{x}_B, \omega)$ is the reflection response measured at surface point \mathbf{x}_A in the presence of an impulsive source at the surface at point \mathbf{x}_B , $T^-(\mathbf{x}_A, \mathbf{x}, \omega)$ is the transmission response measured at the surface point \mathbf{x}_A in the presence of a source at the subsurface point \mathbf{x} at some depth level $\partial\mathcal{D}_m$ and $\mathbf{x}_{H,A}$ stands for the horizontal coordinate vector. If the sources in the subsurface are assumed to be white and uncorrelated, then it can be shown that

$$R^+(\mathbf{x}_A, \mathbf{x}_B, \omega) + \{R^+(\mathbf{x}_A, \mathbf{x}_B, \omega)\}^* = \delta(\mathbf{x}_{H,A} - \mathbf{x}_{H,B}) - T_{obs}^-(\mathbf{x}_A, \omega) \{T_{obs}^-(\mathbf{x}_B, \omega)\}^* , \quad (2)$$

where $T_{obs}^-(\mathbf{x}_A, \omega)$ is transmission response the observed at the surface in the presence of a series of white sources in the subsurface that are acting simultaneously.

Direct migration of white-noise data

After reconstructing the reflection response using one of the above formulas we can use a standard seismic pre-stack or post-stack processing scheme to obtain a reconstructed image of the subsurface. This process was named by Schuster (2001) Interferometric Imag-

ing. Another possibility is to apply migration directly to the transmission data.

If we take as a starting point the formula for downward extrapolation of the reflection response measured at the surface $R^+(\mathbf{x}_A, \mathbf{x}_B, \omega)$

$$R^+(\boldsymbol{\xi}_A, \boldsymbol{\xi}_B, \omega) = \int_{\partial\mathcal{D}_0} \int_{\partial\mathcal{D}_0} \{W^+(\boldsymbol{\xi}_A, \mathbf{x}_A, \omega)\}^* R^+(\mathbf{x}_A, \mathbf{x}_B, \omega) \{W^-(\mathbf{x}_B, \boldsymbol{\xi}_B, \omega)\}^* d\mathbf{x}_A d\mathbf{x}_B, \quad (3)$$

where $R^+(\boldsymbol{\xi}_A, \boldsymbol{\xi}_B, \omega)$ is the reflection response extrapolated to some subsurface level and $W^+(\boldsymbol{\xi}_A, \mathbf{x}_A, \omega)$ and $W^-(\mathbf{x}_B, \boldsymbol{\xi}_B, \omega)$ are forward-extrapolation operators, and we substitute in it equation (2), then it can be shown (Artman et al., 2004) that

$$R^+(\boldsymbol{\xi}_A, \boldsymbol{\xi}_B, \omega) = \text{anti-causal terms} + \int_{\partial\mathcal{D}_0} \{W^+(\boldsymbol{\xi}_A, \mathbf{x}_A, \omega)\}^* T_{obs}^-(\mathbf{x}_A, \omega) d\mathbf{x}_A \left\{ \int_{\partial\mathcal{D}_0} W^+(\boldsymbol{\xi}_B, \mathbf{x}_B, \omega) r T_{obs}^-(\mathbf{x}_B, \omega) d\mathbf{x}_B \right\}^*. \quad (4)$$

In the above equation $r = -1$ is the reflection coefficient of the free surface. Equation (4) shows that by inverse extrapolating the transmission response observed at point \mathbf{x}_A to some depth level, forward extrapolating the back-reflected transmission response observed at point \mathbf{x}_B to the same depth level and then cross-correlating them, one will have the reflection response at this particular level. If we further apply the imaging condition to equation (4), then an image can be built of the subsurface at the point $\boldsymbol{\xi}_A$.

Theory and numerical modelling have shown that the reconstructed depth images using the direct migration of white noise transmission data are identical to the depth images reconstructed by first simulating the reflection response from the observed transmission responses and then migrating the simulated reflection shot panels. The choice of one or the other path of obtaining the depth image depends on the set goals. The direct migration method saves one the necessity for the correlation of the long noise signals, but the extrapolation process itself is also computationally very intense. On the other hand, after reconstructing the reflection responses one needs to preserve only a very short part of interest of the long signal representing the simulated reflection common-shot gather, which makes the subsequent migration process very fast. In the following section the migration images were obtained by first reconstructing the reflection responses for all receiver positions and then migrating them according to

equation (3) combined with the imaging condition.

COMPARISON BETWEEN RECONSTRUCTED REFLECTION RESPONSE AND RECONSTRUCTED DEPTH IMAGE

Theoretical explanation

Let there be a source buried in the subsurface at \mathbf{x}_S and two receivers at the free surface at points \mathbf{x}_A and \mathbf{x}_B (see figure 1a).

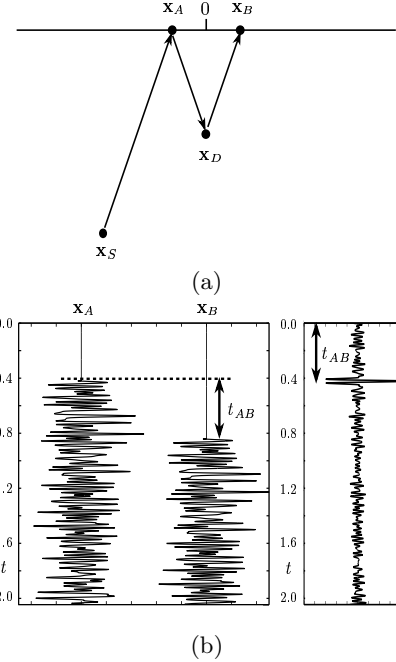


Fig. 1: (a) Example of seismic interferometry with $v = 1500$ m/s, $\mathbf{x}_A = (-100, 0)$, $\mathbf{x}_B = (100, 0)$, $\mathbf{x}_D = (0, 300)$ and $\mathbf{x}_S = (-300, 600)$; (b) If we correlate (left) the direct arrival at \mathbf{x}_A with the scattered arrival at \mathbf{x}_B then we receive a simulated reflection at \mathbf{x}_B (right) as if from an impulsive surface source at \mathbf{x}_A .

A signal emitted from the source is reflected at point \mathbf{x}_A , propagates down to the diffractor and then back to the surface, where it is recorded at \mathbf{x}_B . This is possible when \mathbf{x}_A is at the specular reflection point of the ray that is afterwards recorded at \mathbf{x}_B . The receiver at \mathbf{x}_A records the direct arrival and the receiver at \mathbf{x}_B - the scattered wavefield (see figure 1b (left)).

Cross-correlating the two arrivals will produce a simulated reflection response at \mathbf{x}_B as if coming from an impulsive source at \mathbf{x}_A (figure 1b (right)). This result is possible only in the case of the above mentioned limitations. To overcome these limitations one can make use of multiple sources or of multiple receivers.

In the case of multiple sources (figure 2a) the rays

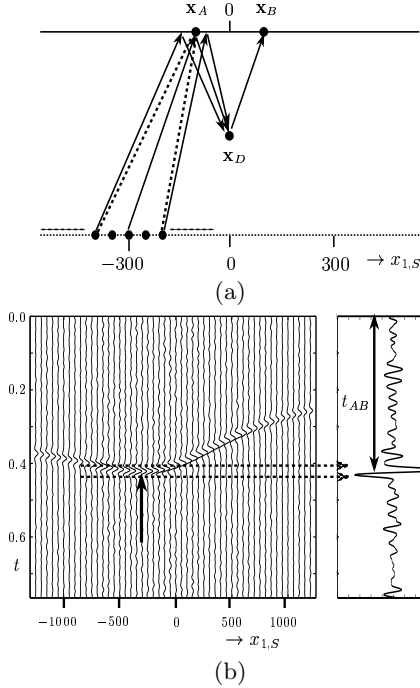


Fig. 2: (a) Example of seismic interferometry with multiple sources; (b) Common receiver panel from the correlated direct arrivals at \mathbf{x}_A with the scattered arrivals at \mathbf{x}_B for each source position (left) and the sum of the correlated traces along $x_{1,S}$ (right).

leaving the sources will follow the solid paths on their way to \mathbf{x}_B . At position \mathbf{x}_A , though, the receiver will record the direct arrivals shown with the dashed lines. The solid and the dashed lines will coincide only for the source from the previous example at $x_{1,S} = -300$.

The results from the correlation of the direct arrivals at \mathbf{x}_A with the scattered arrivals at \mathbf{x}_B are shown in figure 2b (left) as a common receiver gather. The trace at $x_{1,S} = -300$ m shows an impulse at $t = t_{AB}$. The rest of the traces show impulses at earlier times. If now the traces are summed along $x_{1,S}$ then the main contribution in the resulting trace (the trace in figure 2b (right)) will come from the stationary phase zone around the point $x_{1,S} = -300$ indicated with the black vertical arrow. This trace can again be interpreted as the reflection response at \mathbf{x}_B in the presence of an impulsive source at \mathbf{x}_A . From this explanation one can see that the more sources in the subsurface, the better the reconstructed reflection response will be. Note that this is an intuitive explanation of formula (1).

In the case of multiple receivers (figure 3a) the direct arrivals at each receiver position $x_{1,A}$ are forward extrapolated to the diffractor along the dashed lines. The scattered arrivals at \mathbf{x}_B are inversely extrapolated to the diffractor. The result is shown in figure 3b (left) as a common-shot gather.

The trace at $x_{1,A} = -100$ shows an impulse at $t = 0$.

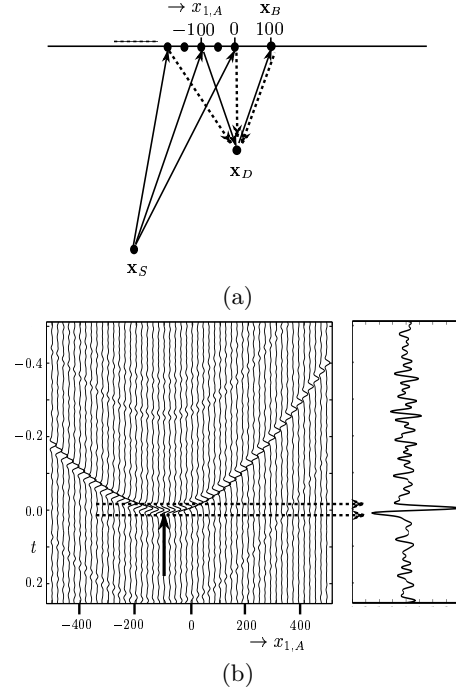


Fig. 3: (a) Example of seismic interferometry with multiple receivers; (b) Common source panel from the extrapolated and consequently correlated direct arrivals at each $x_{1,A}$ with the scattered arrivals at \mathbf{x}_B (left) and the sum of the traces along $x_{1,A}$ (right).

The result from summing all the traces along the horizontal receiver positions $x_{1,A}$ is shown in figure 3b (right). The resulting trace also shows an impulse at $t = 0$. According to the imaging condition in migration, this impulse is placed at the diffractor at \mathbf{x}_D .

From the explanations given above it can be concluded that to reconstruct the reflection response one need to have many subsurface sources (figure 2). When this is not the case, we can instead reconstruct the depth image (figure 3).

Numerical modelling

Figure 4a shows the subsurface model used to model the directly modelled reflection response shown in 4b and the different transmission responses from white-noise sources in the subsurface. One of the traces from the transmission response panels was afterwards cross-correlated according to formula (2) with all other transmission traces to simulate the reflection response from a surface shot with the horizontal position of the chosen trace. At the end all the simulated reflection common-shot gathers were used in a pre-stack shot-profile migration scheme to produce a reconstructed depth image of the subsurface.

As it was shown above, the quality of both the reconstructed reflection response and the reconstructed

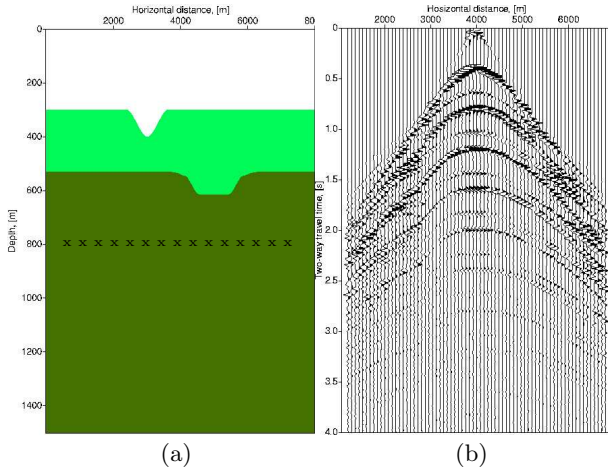


Fig. 4: (a) Double syncline model with white-noise sources at depth level $x_3 = 800$ m; the sources are regularly distributed; the receivers at the surface are distributed between $x_1 = 1200$ and $x_1 = 6800$ m every 20 m; (b) Directly modelled reflection response for the model in (a) with a surface source at $x = (4000, 0)$ m.

depth image depend on the number of the present subsurface sources. Figure 5a through 5d shows the reconstructed reflection response shot gathers with a simulated surface shot position at $x_1 = 4000$ m for a decreasing number of subsurface noise sources. The transmission recordings used to simulate the reflection response were 66 minutes long. One can see that, compared with the directly modelled reflection response from figure 4b, the quality of the simulated reflection response decreases very quickly with decreasing number of the subsurface sources.

Figure 6a through 6d shows the reconstructed depth images obtained from the reconstructed reflection response shot gathers for a decreasing number of subsurface noise sources. One can see that in comparison with the reconstructed reflections, when decreasing the number of subsurface sources, the migration process delivers much better results.

Figure 7a through 7d shows the change in quality of the reconstructed reflection common-shot gathers when shortening the recording time of the transmission responses. For short recording times, the reconstructed reflection hyperbolea can hardly be seen. If, though, the simulated reflection responses are afterwards migrated (figure 8a through 8d) the reconstructed depth image still shows clearly the present subsurface features, only the signal-to-noise ratio has decreased for the shorter recording times.

ELASTIC DAYLIGHT IMAGING

In the appendix of Wapenaar et al. (2004) the extension is given of the acoustic daylight formula (1) for an elastic medium. In the elastic case, in place of the reflection and the transmission responses at the free

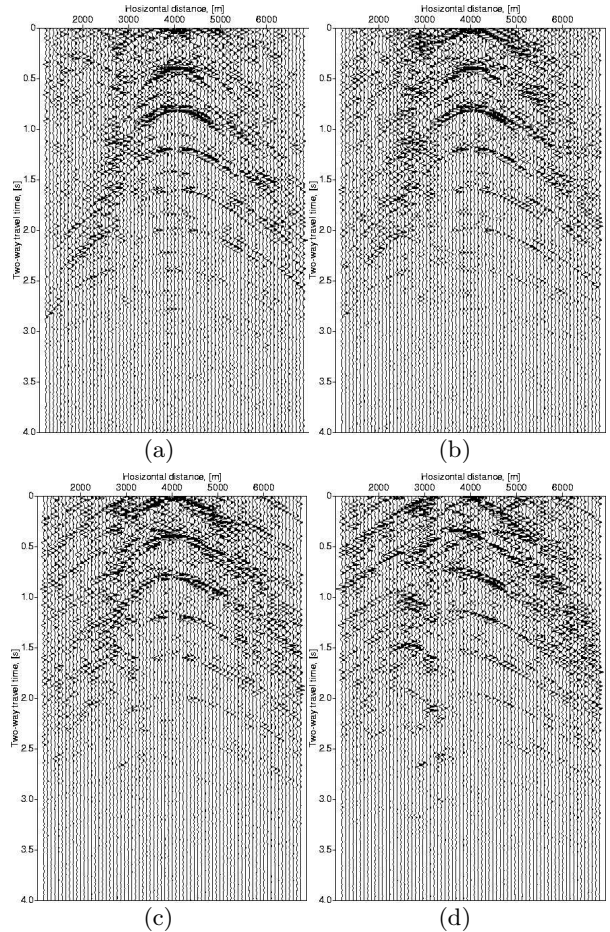


Fig. 5: Reconstructed reflection response common-shot gathers from 66 minutes long noise recordings with (a) 113, (b) 57, (c) 11 and (d) 6 regularly distributed subsurface sources. The simulated surface shot position is at $x_1 = 4000$ m.

surface one has reflection and transmission matrices:

$$\mathbf{R}^+(\mathbf{x}_A, \mathbf{x}_B, \omega) = \begin{pmatrix} R_{\phi, \phi}^+ & R_{\phi, \psi}^+ & R_{\phi, \nu}^+ \\ R_{\psi, \phi}^+ & R_{\psi, \psi}^+ & R_{\psi, \nu}^+ \\ R_{\nu, \phi}^+ & R_{\nu, \psi}^+ & R_{\nu, \nu}^+ \end{pmatrix} (\mathbf{x}_A, \mathbf{x}_B, \omega) \quad (5)$$

and

$$\mathbf{T}^-(\mathbf{x}_A, \mathbf{x}, \omega) = \begin{pmatrix} T_{\phi, \phi}^- & T_{\phi, \psi}^- & T_{\phi, \nu}^- \\ T_{\psi, \phi}^- & T_{\psi, \psi}^- & T_{\psi, \nu}^- \\ T_{\nu, \phi}^- & T_{\nu, \psi}^- & T_{\nu, \nu}^- \end{pmatrix} (\mathbf{x}_A, \mathbf{x}, \omega) . \quad (6)$$

In the above equations ϕ, ψ and ν stand for P- and S-wavefields at the source and at the receiver positions. Then, to simulate the directly modelled reflection response in figure 9 (b) from the transmission response observed at the surface, as shown in figure 9 (a), one has to make use of the elastic daylight imaging equation

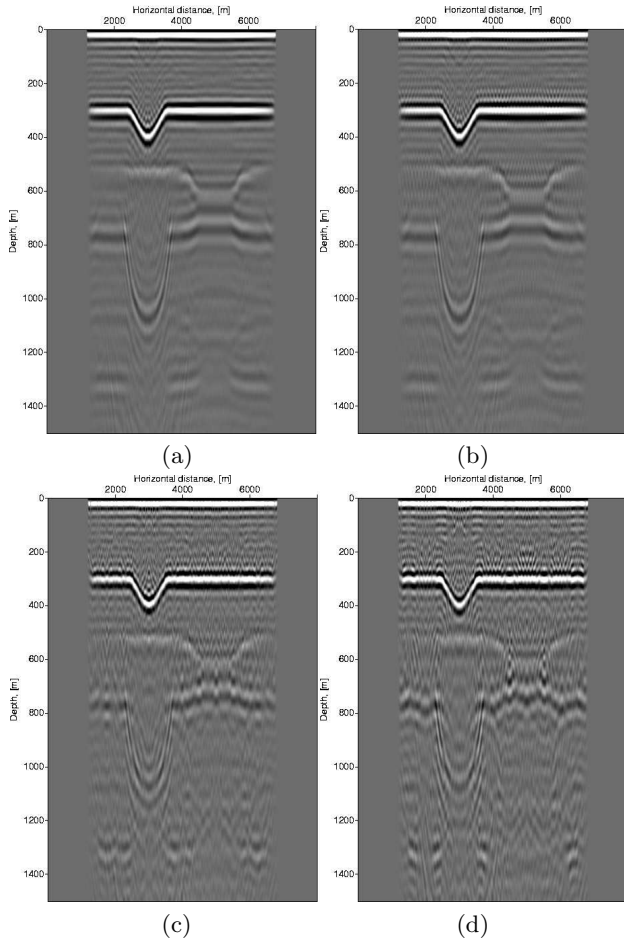


Fig. 6: Reconstructed depth images from migration of the reconstructed reflection response common-shot gathers from 66 minutes long noise recordings with (a) 113, (b) 57, (c) 11 and (d) 6 regularly distributed subsurface sources.

$$\begin{aligned}
& - \hat{\mathbf{r}}^-(\mathbf{x}_A) \mathbf{R}^+(\mathbf{x}_A, \mathbf{x}_B, \omega) \\
& - \{ \mathbf{R}^+(\mathbf{x}_A, \mathbf{x}_B, \omega) \}^* \{ \hat{\mathbf{r}}^-(\mathbf{x}_B) \}^\dagger \\
& = \mathbf{I} \delta(\mathbf{x}_{H,A} - \mathbf{x}_{H,B}) \\
& - \int_{\partial \mathcal{D}_m} \{ \mathbf{T}^-(\mathbf{x}_A, \mathbf{x}, \omega) \}^* \{ \mathbf{T}^-(\mathbf{x}_B, \mathbf{x}, \omega) \}^t d^2 \mathbf{x} .
\end{aligned} \tag{7}$$

In equation (7) \dagger stands for complex conjugate transpose, t for transposition and \mathbf{I} is 3×3 identity matrix. The symbol $\hat{\mathbf{r}}^-(\mathbf{x}_A)$ represents the reflection coefficient operator matrix of the free surface

$$\hat{\mathbf{r}}^-(\mathbf{x}_A) = \begin{pmatrix} \hat{r}_{\phi, \phi}^- & \hat{r}_{\phi, \psi}^- & \hat{r}_{\phi, \nu}^- \\ \hat{r}_{\psi, \phi}^- & \hat{r}_{\psi, \psi}^- & \hat{r}_{\psi, \nu}^- \\ \hat{r}_{\nu, \phi}^- & \hat{r}_{\nu, \psi}^- & \hat{r}_{\nu, \nu}^- \end{pmatrix} (\mathbf{x}_A) , \tag{8}$$

where the symbol $\hat{\cdot}$ denotes a pseudo differential operator acting on the horizontal coordinates .

Equation (7) shows that to reconstruct the reflection response for a certain combination of source and re-

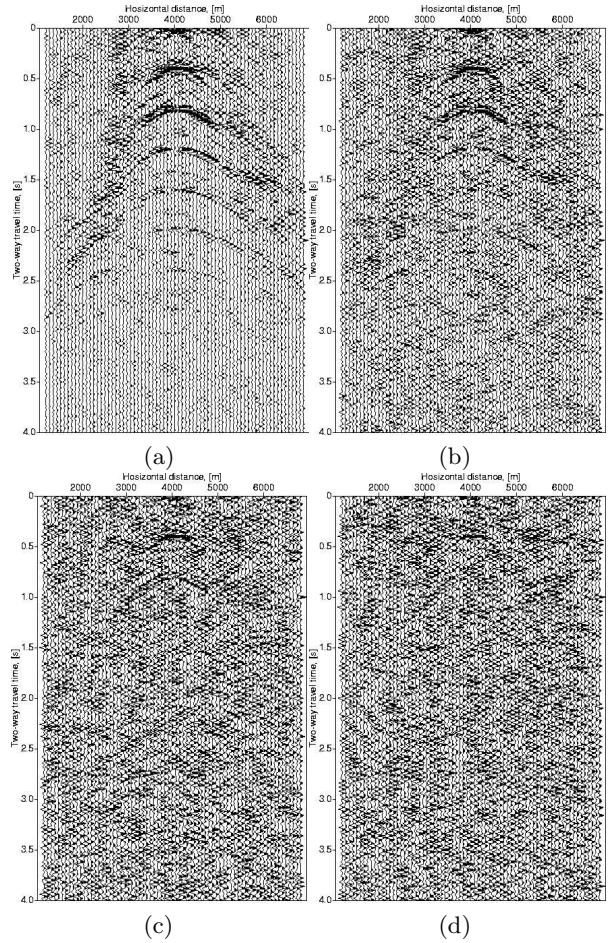


Fig. 7: Reconstructed reflection response common-shot gathers from noise recordings of (a) 33 minutes, (b) 6 minutes, (c) 1 minute and (d) 20 seconds. There were 225 white-noise sources in the subsurface. The simulated surface shot position is at $x_1 = 4000$ m.

ceiver wavefields, the transmission response measured at the surface needs to be decomposed into the different types of P- and S-waves and then cross-correlated. Also, one needs to solve for the reflection coefficients of the free surface for both points \mathbf{x}_A and \mathbf{x}_B .

CONCLUSIONS

By cross-correlating transmission responses the measured at the surface of a 3-D inhomogeneous acoustic medium can reconstruct the reflection response of this medium. To have a good quality simulated reflections one needs to have enough white subsurface noise sources and long recording times. Alternatively, one can migrate the reconstructed reflection response even for a small number of subsurface sources and short registration times - the resulting reconstructed depth image will still be good.

To reconstruct the reflection response from the measured transmission responses in the case of an elastic medium, one needs to decompose the transmission response measured at the surface into P and S one-way wavefields and then perform the cross-

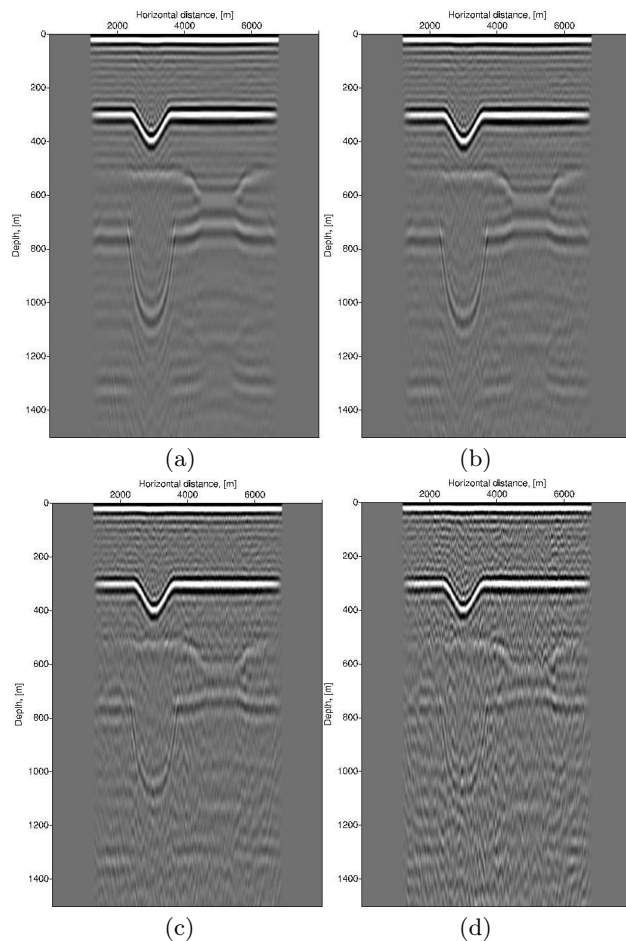


Fig. 8: Reconstructed depth images from migration of the reconstructed reflection response common-shot gathers noise recordings of (a) 33 minutes, (b) 6 minutes, (c) 1 minute and (d) 20 seconds.

correlation. Further, the reflectivity matrix of the free surface need to be solved.

ACKNOWLEDGMENTS

This research is performed as part of research projects financed by the Dutch Science Foundation STW (number DTN4915) and the Dutch Research Centre for Integrated Solid Earth Sciences ISES.

REFERENCES

- Artman, B., Draganov, D., Wapenaar, C. P. A., and Biondi, B., 2004, Direct migration of passive seismic data: 66th Conf. and Exhib., Europ. Assoc. Geosc. Eng., Extended abstracts P075.
- Claerbout, J. F., 1968, Synthesis of a layered medium from its acoustic transmission response: *Geophysics*, 33.
- Schuster, G. T., 2001, Theory of daylight/interferometric imaging: tutorial: 63th Conf. and Exhib., Europ. Assoc. Geosc. Eng., Extended abstracts A-32.

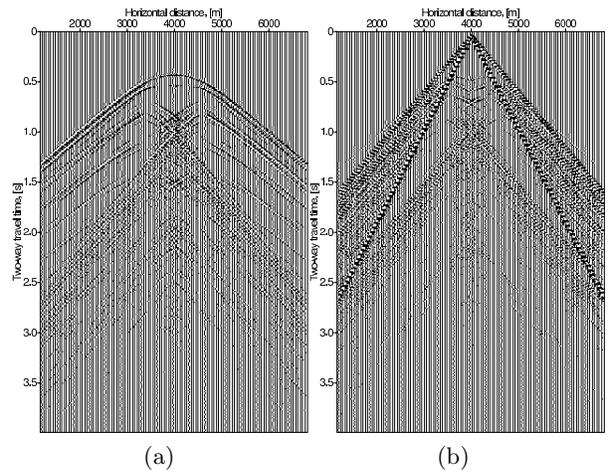


Fig. 9: (a) Modelled transmission P-recording at the surface for a syncline model with one subsurface impulsive P-source; (b) Directly modelled reflection P-recording at the surface for the same model with an impulsive P-source at the surface.

Wapenaar, C. P. A., Thorbecke, J. W., Draganov, D., and Fokkema, J. T., 2002, Theory of acoustic daylight imaging revisited: 72nd Ann. Internat. Mtg., Soc. Expl. Geophys., Expanded abstracts ST 1.5.

Wapenaar, C. P. A., Thorbecke, J. W., and Draganov, D., 2004, Relations between reflection and transmission responses of 3-D inhomogeneous media: *Geophys. J. Int.*, 156, 179–194.